A Journal of the Gesellschaft Deutscher Chemiker
Angewandte Chemie
GDCh
International Edition
www.angewandte.org

Accepted Article

Title: Dearomatizing [4+1] Spiroannulation of Naphthols: Discovery of Structurally Non-Traditional Thermally Activated Delayed Fluorescent Materials

Authors: Wenbo Liang, Yudong Yang, Mufan Yang, Min Zhang, Chengming Li, You Ran, Jingbo Lan, Zhengyang Bin, and Jingsong You

To be cited as: *Angew. Chem. Int. Ed.* 10.1002/anie.202012842

Link to VoR: https://doi.org/10.1002/anie.202012842

WILEY-VCH

Dearomatizing [4+1] Spiroannulation of Naphthols: Discovery of Structurally Non-Traditional Thermally Activated Delayed Fluorescent Materials

Wenbo Liang, Yudong Yang, Mufan Yang, Min Zhang, Chengming Li, You Ran, Jingbo Lan, Zhengyang Bin,* and Jingsong You*

[*] W. Liang, Prof. Dr. Y. Yang, M. Yang, M. Zhang, Dr. C. Li, Y. Ran, Prof. Dr. J. Lan, Prof. Dr. Z. Bin, Prof. Dr. J. You
Key Laboratory of Green Chemistry and Technology of Ministry of Education
College of Chemistry, Sichuan University
29 Wangjiang Road, Chengdu 610064, People's Republic of China
E-mail: binzhengyang@scu.edu.cn, jsyou@scu.edu.cn

Supporting information for this article is given via a link at the end of the document.

Abstract: The development of streamlined synthetic routes to spirofluorene derivatives, in particular those with a donor-acceptor (D-A) system, is an appealing task in the field of organic functional materials. In this work, we disclose a palladium-catalyzed direct [4+1] spiroannulation of *ortho*-C−H bonds of naphthols with cyclic diaryliodonium salts to construct spirofluorenyl naphthalenones (SFNP) under mild reaction conditions. This spiroannulation not only directly transforms the hydroxyl group into the carbonyl group, but also tolerates reactive functional groups such as the halo groups, which provide an opportunity to rapidly assemble structurally non-traditional thermally activated delayed fluorescent (TADF) materials that feature a carbonyl group with an adjacent spirofluorenyl unit as the acceptor. As an illustrated example, the OLED device utilizing the assembled **DMAC-SFNP** as the host material exhibits a low turn-on voltage of 2.5 V and an ultra-high external quantum efficiency of 32.2%. This work not only gives us an inspiration for designing structurally non-traditional TADF materials, but also displays the charm of C−H activation as a revolutionary synthetic strategy in the innovation of optoelectronic materials.

C−H bond activation is referred to the “holy grail” of organic synthesis. The direct transformation of ubiquitous C−H bonds not only provides unusual strategic disconnections for the construction of hard-to-form bonds but also enables the rapid assembly of complex structures from simple substrates with excellent functional group tolerance.[1] Consequently, this revolutionary synthetic strategy is believed to fuel the innovation of organic functional materials and pharmaceuticals.[2]

Spirocyclic aromatic compounds have drawn tremendous attentions for their broad applications in organic optoelectronic materials, such as organic light emitting diodes (OLEDs) and organic solar cells (OSCs).[3] In particular, the spirofluorene derivatives featuring a donor-acceptor (D-A) system are one of the most anticipated structures for OLED host materials, because of their balanced carrier transporting property, high triplet energy level and good thermal stability.[4] However, conventional synthetic approaches to the spirofluorenyl structures typically require multiple steps and the use of highly reactive organometallic reagents (e.g., Grignard reagent and *n*-butyllithium), which restrict the diversity of molecular skeletons and further exploration of novel materials (Scheme 1a).[5] Thus, the development of general and concise methods to overcome the above limitations and enable rapid diversification of spirofluorenes is highly desired.

In recent years, transition metal-catalyzed dearomatization *via* C−H activation has emerged as a powerful approach to spirocycles.[6] In this regard, the dearomatizing spiroannulation of phenol derivatives is particularly intriguing because it allows the incorporation of a carbonyl group into the resulting spirocyclic products. It is worthy of note that the carbonyl group is usually employed to form an acceptor unit in organic optoelectronic molecules.[7] Recently, the dearomatizing [3+2] spiroannulation of naphthol-based biaryls with alkynes, and [2+2+1] spiroannulation of bromonaphthols with aryl iodides and alkynes have been established to access spiroindenyl naphthalenones (Scheme 1b).[6b,6e,8] Inspired by these elegant works, we reasoned that spirofluorenyl naphthalenones could be assembled by [4+1] spiroannulation of naphthols with aryl equivalents instead of alkynes (Scheme 1c). Cyclic diaryliodonium salts have been employed as biarylation reagents in the transition metal-catalyzed [4+2] annulation reactions for the construction of π-fused aromatic materials.[9] Herein we present a palladium-catalyzed direct [4+1] spiroannulation of *ortho*-C−H bonds of naphthols with cyclic diaryliodonium salts, which enables the streamlined synthesis of spirofluorenyl naphthalenones and rapid assembly of structurally non-traditional TADF materials.

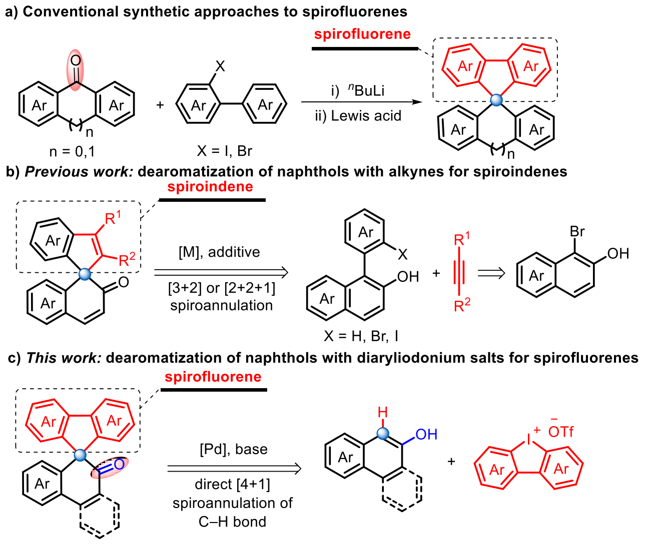

Scheme 1. Synthesis of spirocyclic derivatives.

The dearomatizing spiroannulation of 2-naphthol with cyclic diphenyliodonium salt was investigated through palladium catalysis (Table 1). After screening of a variety of parameters, including palladium sources, bases, solvents and temperature, the reaction of **1a** with **2a** afforded the desired spirofluorene **3aa** in 91% isolated yield at 60 °C (Table 1, entry 1). Control experiments demonstrated that palladium catalyst and base were indispensable (Table 1, entries 2 and 3). The replacement of $Pd_2(dba)_3$ with $Pd(PPh_3)_4$, $[Pd(C_3H_5)Cl]_2$ or $Pd(OAc)_2$ resulted in inferior efficiencies (Table 1, entries 4 and 5). Other solvents such as toluene, DCE, 1,4-dioxane, HFIP and DMF were less effective than TFE (Table 1, entries 6 and 7). Other bases (e.g., Cs_2CO_3 and K_2CO_3) gave slightly low yields (Table 1, entry 8). In addition, the C−O coupling product was not detected in this transformation although diaryliodonium salts are easily attacked by nucleophilic reagents.[9a] The replacement of **2a** with 2,2'-diiodo-1,1'-biphenyl did not yet give the desired product.

Table 1. Optimization of the reaction conditions.[a]

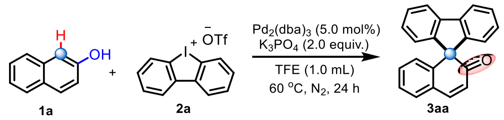

Entry	Variation from the standard conditions	Yield [%][b]
1	none	96 (91)[c]
2	without $Pd_2(dba)_3$	N.R.
3	without K_3PO_4	N.R.
4	$Pd(PPh_3)_4$ instead of $Pd_2(dba)_3$	68
5	$[Pd(C_3H_5)Cl]_2$ or $Pd(OAc)_2$ instead of $Pd_2(dba)_3$	88, 67
6	toluene, DCE, dioxane instead of TFE	45, 41, 28
7	HFIP or DMF instead of TFE	10, trace
8	Cs_2CO_3, K_2CO_3 instead of K_3PO_4	89, 87

[a] Reaction conditions: **1a** (0.2 mmol), **2a** (0.4 mmol), $Pd_2(dba)_3$ (5.0 mol%), K_3PO_4 (2.0 equiv) and TFE (1.0 mL) at 60 °C for 24 h under N_2. [b] NMR yield using dibromethane as an internal standard. [c] Isolated yield in parentheses. DCE = 1,2-dichloroethane, HFIP = 1,1,1,3,3,3-hexafluoroisopropanol, DMF = *N*,*N*-dimethylformamide, TFE = 2,2,2-trifluoroethanol.

With the optimized reaction conditions in hand, the substrate scope with regard to 2-naphthols **1** was examined. As shown in Scheme 2, a range of 2-naphthols smoothly underwent the spiroannulation reaction with **2a** to deliver spirofluorenyl naphthalenones **3** in moderate to excellent yields (**3aa**-**3pa**). In comparison with the conventional synthetic approaches to spirofluorenes from fluorenones and organometallic reagents,[5] this protocol tolerated a broad scope of functional groups, including methyl, phenyl, 1-naphthyl, benzyloxy, methoxy, 2-thienyl, and even ester, formyl, cyano, bromo and chloro (**3ba-3na, 3pa**). The excellent functional group compatibility of this reaction is highly important for further construction of functional molecules. To demonstrate the synthetic applicability of this reaction, a 1.0 mmol scale reaction was conducted, delivering **3la** in 80% yield. Moreover, 9-phenanthrol and 6-chlorophenanthren-9-ol also underwent this transformation to provide the desired products in moderate yields (**3oa** and **3pa**).

Next, the scope of cyclic diaryliodonium salts **2** was explored (Scheme 2). The symmetrical cyclic diaryliodonium salts with various substituents, such as methyl, *t*-butyl, phenyl, methoxy, trifluoromethyl, fluoro and chloro, at either *para* or *meta* position could react with 2-naphthol to afford the dearomatized products (**4ab−4aj**, and **4kg**). The reactions with nonsymmetrical cyclic diaryliodonium salts enabled the synthesis of unsymmetrical spirofluorene derivatives (**4ak−4am**). The sterically hindered **2m** gave a relatively low yield of 41% with accompany of the recovery of **1a** in 52% yield. The excessive cyclic diaryliodonium salt **2m** was decomposed completely after the reaction. Besides, the structures of **3fa** and **4am** were demonstrated by the X-ray single crystal analysis (Part V, SI).[10]

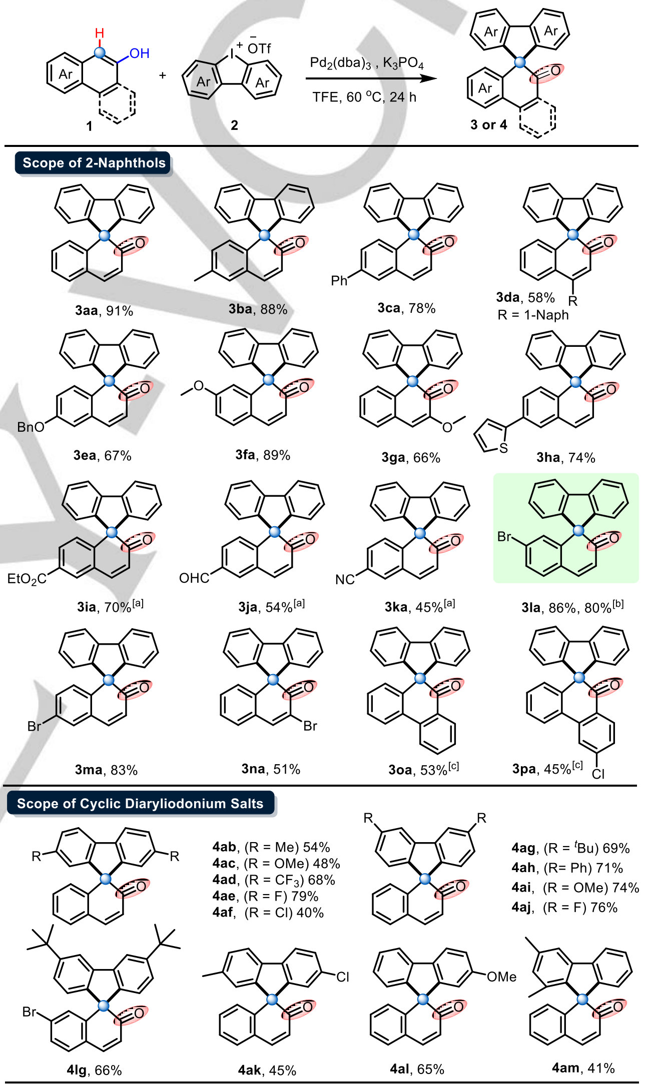

Scheme 2. Scope of substrates. Reaction conditions: **1** (0.2 mmol), **2** (0.4 mmol), $Pd_2(dba)_3$ (5.0 mol%), K_3PO_4 (2.0 equiv) and TFE (1.0 mL) at 60 °C for 24 h under N_2. Isolated Yields. [a] 80 °C. [b] 1.0 mmol scale. [c] 40 °C.

Recently, the TADF materials featuring a donor−acceptor structure have attracted much attention in the field of OLEDs because they can theoretically realize 100% internal quantum efficiency.[11] With a library of spirofluorenyl naphthalenones (SFNP) in hand, we tried to assemble the TADF molecule (**DMAC-SFNP**) using widely used 9,9-dimethyl-9,10-dihydroacridine (DMAC) as the donor (Figure 1a). The spiroannulation developed herein is tolerant of the reactive bromo group, which provides a streamlined route to the bromocontaining precursor **3la** for the subsequent Buchwald–Hartwig amination with DMAC (for details, see Part IX, SI). The theoretical calculations demonstrate that the lowest unoccupied molecular orbitals (LUMO) of **DMAC-SFNP** are mainly localized on the electron-deficient naphthalenone plane, while the highest occupied molecular orbitals (HOMO) are mostly distributed over the electron-rich DMAC donor (Figure 1b). Therefore, small overlap of the frontier orbitals (FMOs) leads to a tiny singlet-triplet energy gap (ΔE_{ST}) of 0.013 eV, indicating the potential of spirofluorenyl naphthalenones for designing TADF materials (Figure 1c). To investigate the effect of π-π stacking between the fluorene units on OLED performance, **DMAC-^{t}BuSFNP** with two sterically hindered *tert*-butyl groups on the fluorene unit is designed for comparison (Figure 1a). Because the spiro quaternary carbon center disrupts the π-conjugation between the fluorene and napthalenone units, the LUMO distributions of the compounds are not delocalized to the fluorene unit (Figure 1b). Therefore, we proposed that the introduction of electron-donating *t*-butyl group on the fluorene unit would slightly influence the electrochemical and photophysical properties of molecules, which could be demonstrated by the same FMOs energy levels of **DMAC-SFNP** and **DMAC-^{t}BuSFNP** (-5.10 eV for HOMO, and -2.38 eV for LUMO) (Figure S3) and the similar emission peaks in the fluorescence spectra (527 nm for **DMAC-SFNP**, and 524 nm for **DMAC-^{t}BuSFNP**) (Figure S4).

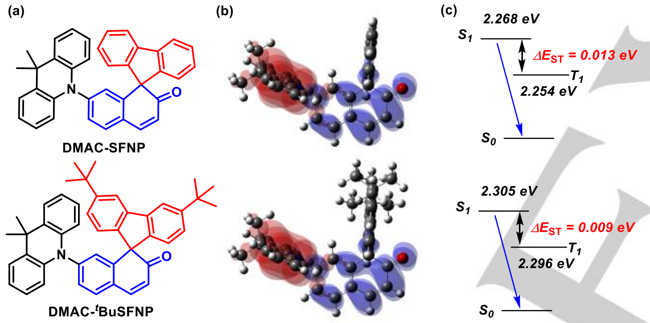

Figure 1. a) Molecular structures, b) theoretical LUMO (blue)/HOMO (red) distributions and c) calculated energy levels of **DMAC-SFNP** (top) and **DMAC-^{t}BuSFNP** (bottom).

To examine the TADF characteristics of **DMAC-SFNP** and **DMAC-^{t}BuSFNP**, the UV-*vis* absorption and photoluminescence (PL) spectra were measured (Part XII, SI). In the absorption spectra (Figure S4), a broad absorption band appears in the region of 350-450 nm for **DMAC-SFNP** and **DMAC-^{t}BuSFNP**, which is attributed to charge-transfer absorption from the DMAC donor to the SFNP acceptor. The fluorescence spectra were measured in 4,4'-bis(N-carbazolyl)biphenyl (CBP) host at room temperature, and the phosphorescence spectra were measured at 77 K. The singlet energies (E_{S1}) and triplet energies (E_{T1}) were calculated to be 2.62 eV and 2.35 eV for **DMAC-SFNP**, and 2.63 eV and 2.31 eV for **DMAC-^{t}BuSFNP**, exhibiting small ΔE_{ST} values of 0.27 eV and 0.32 eV, respectively. The transient PL spectra also displayed obvious delayed PL characteristics with average lifetimes of 88.6 μs and 53.7 μs for **DMAC-SFNP** and **DMAC-^{t}BuSFNP**, respectively, indicating the TADF behaviour (Figure S5 and Table S3).

The crystal X-ray structures and packing patterns of **DMAC-SFNP** and **DMAC-^{t}BuSFNP** are shown in Figure 2.[10] The two compounds show similar structures with large dihedral angels of 86.55° and 89.98° between the fluorene and naphthalene units, and 67.78° and 80.85° between the DMAC donor and the SFNP acceptor. However, as predicted, their packing patterns are quite different. In the crystal of **DMAC-SFNP**, π-π interactions with distances of 3.57 Å between the fluorene units are found. The DMAC donors are also well-packed with the distance of 3.80 Å *via* intermolecular π-π stacking interaction (Figure 2c). This compact and ordered face-to-face packing mode would provide a favourable condition for effective carrier transport between the neighbouring molecules and potentially enable **DMAC-SFNP** a superior candidate for TADF host material. In contrast, the significant steric hindrance of *t*-butyl groups prevents the close interaction between the neighbouring spiro fluorene units in the crystal of **DMAC-^{t}BuSFNP**, and thus changes the packing structure to an unordered tail-to-tail mode with the interaction among *t*-butyl groups (Figure 2d), which is unfavoured for carrier transport.

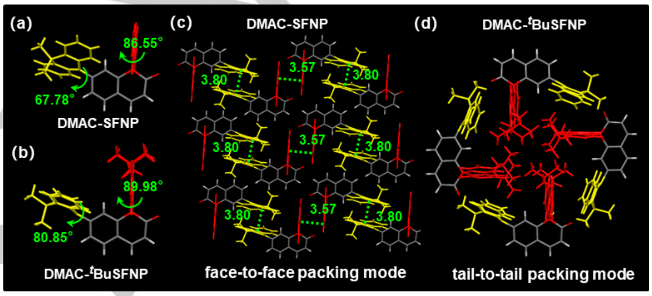

Figure 2. Crystal structures of a) **DMAC-SFNP** and b) **DMAC-^{t}BuSFNP**. Packing structures of c) **DMAC-SFNP** and d) **DMAC-^{t}BuSFNP**.

OLED devices were fabricated using **DMAC-SFNP** and **DMAC-^{t}BuSFNP** as the host materials and ($Ir(mphmq)_2(tmd)$) as the emitter in the emitting layers. The widely used diaryl ketone TADF host material **DMAC-BP** was used for comparison (Figure 3).[12] All the devices show similar emission spectra with emission peak at 605 nm, indicating the sufficient energy transfer from host material to $Ir(mphmq)_2(tmd)$ emitter. Although **DMAC-SFNP** and **DMAC-^{t}BuSFNP** possess similar photophysical and electrochemical properties, the device performances are considerably different. For example, the turn-on voltage (V_{on}) of **DMAC-SFNP**-based device is only 2.5 V and the maximum external quantum efficiency (EQE_{max}) is as high as 32.2%, which are significantly superior to those of **DMAC-^{t}BuSFNP**-based devices (4.1 V and 18.5%). Compared with the highly efficient **DMAC-BP** host, **DMAC-SFNP**-based device could even possess a better device performance with a lower turn-on voltage (2.7 V for **DMAC-BP**) and a largely enhanced efficiency (21.2% for **DMAC-BP**). Moreover, the current density of **DAMC-SFNP**-based device is significantly higher than that of **DMAC-^{t}BuSFNP**-based devices, which further demonstrates that the planar conformation of fluorene unit is quite important to ensure the compact and ordered face-to-face packing mode, which enhances device performances.

In conclusion, we have developed a dearomatizing [4+1] C−H spiroannulation of naphthols with cyclic diaryliodonium salts for the rapid assembly of spirofluorenyl naphthalenones, which are further used as the acceptor to construct structurally non-traditional TADF materials. The merging of fluorene units leads to effective face-to-face packing, thus achieving high-performance OLEDs. This work demonstrates the superiority of spirofluorenyl naphthalenone bifunctional skeleton for constructing efficient TADF materials.

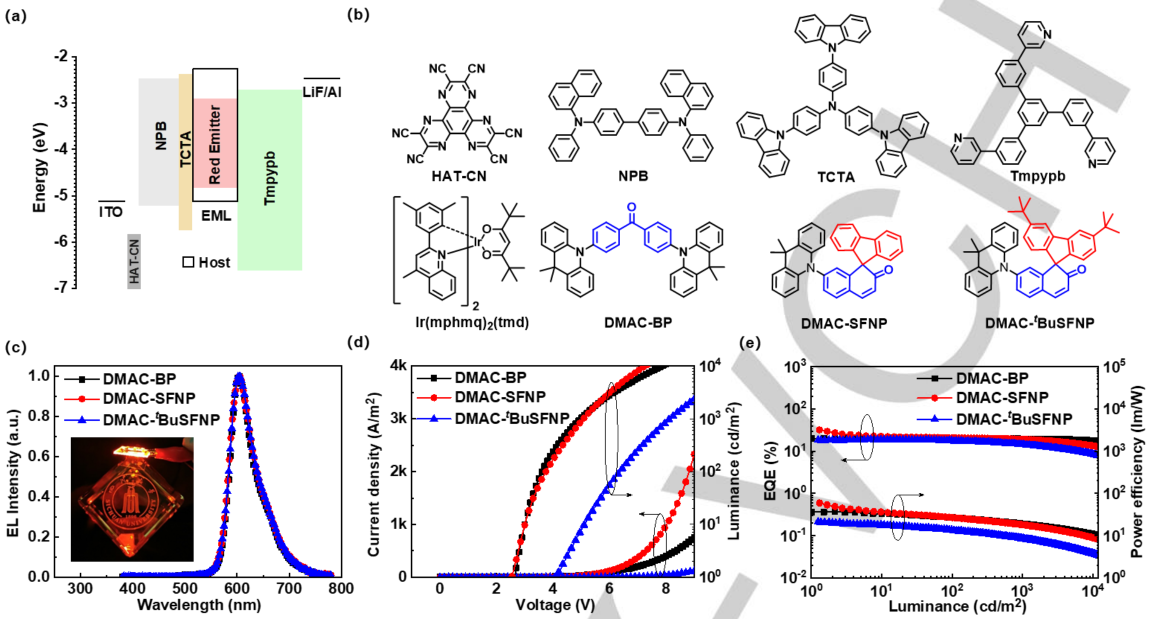

Figure 3. a) Device structure and energy-level diagram of OLED devices. Optimized device structure: ITO/HATCN (5 nm)/NPB (30 nm)/TCTA (10 nm)/Ir(mphmq)$_2$(tmd):TADF host (3%, 25 nm)/Tmpypb (50 nm)/LiF (0.8 nm)/Al (100 nm); b) Molecular structures used in OLED devices; c) EL spectra at the luminance of 1000 cd/m^2; d) Luminance and current density versus voltage curves; and e) EQE and power efficiency versus luminance curves of OLED devices.

Acknowledgements

We acknowledge financial support from the National NSF of China (No 22031007).

Keywords: C−H activation • spiroannulation • dearomatization • thermally activated delayed fluorescence

[1] a) J. Wencel-Delord, F. Glorius, *Nat. Chem.* **2013**, *5*, 369; b) J. He, M. Wasa, K. S. L. Chan, Q. Shao, J.-Q. Yu, *Chem. Rev.* **2017**, *117*, 8754.

[2] a) Y. Segawa, T. Maekawa, K. Itami, *Angew. Chem.* **2015**, *127*, 68; *Angew. Chem. Int. Ed.* **2015**, *54*, 66; b) T. Cernak, K. D. Dykstra, S, Tyagarajan, P, Vachalb, S. W. Krska, *Chem. Soc. Rev.* **2016**, *45*, 546; c) Y. Yang, J. Lan, J. You, *Chem. Rev.* **2017**, *117*, 8787; d) I. A. Stepek, K. Itami, *ACS Mater. Lett.* **2020**, *2*, 951; e) Y. Cheng, G. Li, Y. Liu, Y. Shi, G. Gao, D. Wu, J. Lan, J. You, *J. Am. Chem. Soc.* **2016**, *138*, 4730; f) K. Xu, Y. Fu, Y. Zhou, F. Hennersdorf, P. Machata, I. Vincon, J. J. Weigand, A. A. Popov, R. Berger, X. Feng, *Angew. Chem.* **2017**, *129*, 16092; *Angew. Chem. Int. Ed.* **2017**, *56*, 15876; g) S. D. Friis, M. J. Johansson, L. Ackermann, *Nat. Chem.* **2020**, *12*, 511; h) Z. Huang, Z. Bin, R. Su, F. Yang, J. Lan, J. You, *Angew. Chem.* **2020**, *132*, 10078; *Angew. Chem. Int. Ed.* **2020**, *59*, 9992.

[3] a) T. P. I. Saragi, T. Spehr, A. Siebert, T. Fuhrmann -Lieker, J. Salbeck, *Chem. Rev.* **2007**, *107,* 1011; b) C. Poriel, J. Rault-Berthelot, *J. Mater. Chem. C* **2017**, *5,* 3869; c) G. Méhes, H. Nomura, Q. Zhang, T. Nakagawa, C. Adachi, *Angew. Chem.* **2012**, *124,* 11473; *Angew. Chem., Int. Ed.* **2012**, *51,* 11311; d) L.-S. Cui, Y.-M. Xie, Y.-K. Wang, C. Zhong, Y.-L. Deng, X.-Y. Liu, Z.-Q. Jiang, L.-S. Liao, *Adv. Mater.* **2015**, *27,* 4213; e) N. J. Jeon, H. Na, E. H. Jung, T.-Y. Yang, Y. G. Lee, G. Kim, H.-W. Shin, S. Il Seok, J. Lee, J. Seo, *Nat. Energy*, **2018**, *3*, 682.

[4] a) Y.-K. Wang, Q. Sun, S.-F. Wu, Y. Yuan, Q. Li, Z.-Q. Jiang, M.-K. Fung, L.-S. Liao, *Adv. Funct. Mater.* **2016**, *26*, 7929; b) Y.-K. Wang, S.-H. Li, S.-F. Wu, C.-C. Huang, S. Kumar, Z.-Q. Jiang, M.-K. Fung, L.-S. Liao, *Adv. Funct. Mater.* **2018**, *28,* 1706228; c) C. Han, Z. Zhang, D. Ding, H. Xu, *Chem* **2018**, *4*, 2154.

[5] a) L.-H. Xie, J. Liang, J. Song, C.-R. Yin, W. Huang, *Curr. Org. Chem.* **2010**, *14,* 2169; b) M. Romain, D. Tondelier, J.-C. Vanel, B. Geffroy, O. Jeannin, J. Rault-Berthelot, R. Metivier, C. Poriel, *Angew. Chem.* **2013**, *125,* 14397; *Angew. Chem. Int. Ed.* **2013**, *52*, 14147.

[6] a) I. Khan, A. Ibrar, S. A. Shehzadi, *Coord. Chem. Rev.* **2019**, *380*, 440; b) J. Nan, Z. Zuo, L. Luo, L. Bai, H. Zheng, Y. Yuan, J. Liu, X. Luan, Y. Wang, *J. Am. Chem. Soc.* **2013**, *135*, 17306; c) A. Seoane, N. Casanova, N. Quiñones, J. L. Mascareñas, M. Gulías, *J. Am. Chem. Soc.* **2014**, *136*, 7607; d) S. Kujawa, D. Best, D. J. Burns, H. W. Lam, *Chem. Eur. J.* **2014**, *20*, 8599; e) J. Zheng, S.-B. Wang, C. Zheng, S.-L. You, *J. Am. Chem. Soc.* **2015**, *137,* 4880.

[7] Z. Yang, Z. Mao, Z. Xie, Y. Zhang, S. Liu, J. Zhao, J. Xu, Z. Chi, M. P. Aldred, *Chem. Soc. Rev.* **2017**, *46*, 915.

[8] a) W.-T. Wu, L. Zhang, S.-L. You, *Chem. Soc. Rev.* **2016**, *45*, 1570; b) J. An, M. Bandini, *Eur. J. Org. Chem.* **2020**, 4087; c) L. Yang, H. Zheng, L. Luo, J. Nan, J. Liu, Y. Wang, X. Luan, *J. Am. Chem. Soc.* **2015**, *137,* 4876; d) Z. Zuo, H. Wang, L. Fan, J. Liu, Y. Wang, X. Luan, *Angew. Chem.* **2017**, *129*, 2811; *Angew. Chem., Int. Ed.* **2017**, *56,* 2767; e) Z. Zuo, J. Wang, J. Liu, Y. Wang, X. Luan, *Angew. Chem.* **2020**, *132*, 663; *Angew. Chem. Int. Ed.* **2020**, *59*, 653. For the evaluation of aromatic stabilization energies, see: f) P. von Ragué Schleyer, F. Pühlhofer, *Org. Lett.* **2002**, *4*, 2873.

[9] a) N. Chatterjee, A. Goswami, *Eur. J. Org. Chem*. **2017**, 3023; b) B. P. Mathew, H. J. Yang, J. Kim, J. B. Lee, Y.-T. Kim, S. Lee, C. Y. Lee, W. Choe, K. Myung, J.-U. Park, S. Y. Hong, *Angew. Chem.* **2017**, *129*, 5089; *Angew. Chem. Int. Ed.* **2017**, *56,* 5007.

[10] CCDC 2025134 (**3fa**), 2021738 (**4am**), 2021739 (**DMAC-SFNP**) and 2021740 (**DMAC-ᵗBuSFNP**) contains the supplementary crystallographic data for this paper. These data can be obtained free of charge from The Cambridge Crystallographic Data Centre.

[11] M. Y. Wong, E. Z.-Colman, *Adv. Mater.* **2017**, *29*, 1605444.

[12] Q. Zhang, D. Tsang, H. Kuwabara, Y. Hatae, B. Li, T. Takahashi, S. Y. Lee, T. Yasuda, C. Adachi, *Adv. Mater.* **2015**, *27,* 2096.

Entry for the Table of Contents

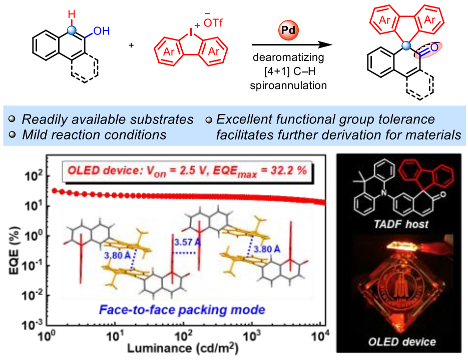

Synthetic strategy unlocks novel optoelectronic materials: A dearomatizing [4+1] C−H spiroannulation of naphthols with cyclic diaryliodonium salts has been developed to rapidly deliver spirofluorenyl naphthalenones, which unlocks an opportunity to discover structurally non-traditional TADF materials.